



Development of Green Engineered Cementitious Composite using Fly Ash and Nanosilica for 3D Printing

S. Anandaraj^{1*}, S. Sakthi Sowmya², A. R. Krishnaraja² and T. Mithun²

¹Department of Civil Engineering, KPR Institute of Engineering and Technology, Coimbatore, TN, India

²Department of Civil Engineering, Kongu Engineering College, Perundurai, TN, India

Received: 09.02.2024 Accepted: 19.3.2024 Published: 30.03.2024

*umailanandkrish@gmail.com

ABSTRACT

The effects of adding Nanosilica (NS) to Engineered Cementitious Composites (ECC) for 3D Printing (3DP) applications were investigated in this study. The mechanical characteristics of 3DP ECC mortar with different NS contents were investigated. The basic components of the composite included fly ash, M-sand, polypropylene fibers, Ordinary Portland Cement, nanosilica and an accelerator. There were four different mix proportions of NS involving 0.05%, 0.1%, 0.15%, and 0.2%. After 3, 7, 14, and 28 days of curing, the following strengths, viz., pull-out strength, direct tensile strength, compressive strength, and flexural strength were assessed. Addition of NS improved the mechanical properties of ECC up to an ideal level of 0.15%, after which decreasing returns and adverse effects, including agglomeration, were observed. Insights into the ideal NS content for obtaining maximum performance of ECC obtained from the study provide knowledge for formulations in high-performance 3DP technologies.

Keywords: Nanosilica; Compressive strength; Flexural strength; Tensile strength; Pull-out strength; 3D Printing.

1. INTRODUCTION

The use of 3D printing technology has a significant impact on recent advancements in the construction industry. This technology has several advantages including, increased design freedom, quicker construction, and minimized material waste (Buswell *et al.* 2020; Huang *et al.* 2023; Sun *et al.* 2021). Well prepared engineered cementitious composites with outstanding printing properties are necessary for the 3D Printing technology to work effectively. Often, the printed compounds in practical applications are cement-based materials. Recent studies have explored mechanical properties of various materials used in 3DP (Fang *et al.* 2023; Wan *et al.* 2023; Zhang *et al.* 2023). Due to its better mechanical properties and low cost, concrete has been used extensively in construction. Its low tensile strength and brittleness, however, present difficulties that need regular maintenance and inspections. Integrating fibers into concrete has been the focus of research to improve its performance. (Afroughsabet and Teng, 2020). Engineered Cementitious Composites (ECC) are a kind of fiber-reinforced concrete known for their unique strain-hardening characteristics and remarkable ductility (Ji *et al.* 2023). With a focus on cementitious materials rather than coarse aggregates, ECC, developed based on micromechanical principles, have been gradually employed for practical engineering applications

improving productivity (Wasim *et al.* 2022; Zhang *et al.* 2022). To reduce the environmental effect of cement manufacturing and protect natural resources, fly ash, a byproduct of burning coal, is frequently used as a cementitious ingredient in concrete (Eřtoková *et al.* 2022). Thermoplastic polymers, including polypropylene (PP) fibers, because of their adaptability, durability, and resistance to chemicals and environmental variables, are frequently employed in a variety of applications (Malchiodi *et al.* 2023; Nazar *et al.* 2023). Polypropylene is frequently added to concrete as an additive in the engineering and construction fields to improve its longevity, reduce cracking, and increase tensile strength (Várdai *et al.* 2020). It is well known that PP fibers could strengthen concrete and enhance its functionality in a variety of situations (Ferdinánd *et al.* 2023). Recently, researchers have been paying more attention to nano-engineered materials, especially NS, which are widely used in cement-based materials (Elkady *et al.* 2013; Wu *et al.* 2017; Yang *et al.* 2021). Having high specific surface area and pozzolanic reactivity, NS improved the mechanical characteristics, durability, and hydration behaviour of cement composites. A suitable quantity of NS was found to greatly improve the mechanical behaviour of the cement fiber reinforced systems in addition to the mechanical properties of plain concrete. Additionally, NS has been shown to successfully improve the bonding between the fibers and the matrix (Lu *et al.* 2018).

2. MATERIALS AND METHODOLOGY

2.1. Cementitious Materials

The Ordinary Portland Cement (OPC) grade 53 was used here as a binder. It obeys IS 8112-2013. It was procured from Priya cements, India. The chemical components of the cement are listed in Table 1. Characteristics of cement determined through preliminary tests are listed in Table 2.

The fly ash belonging to class F was used here. It was procured from Mettur thermal power plant, Tamil Nadu, India. The chemical components of fly ash are listed in Table 1. The physical characteristics of the fly ash were tested in accordance with Indian (Table 3).



Fig. 1: Nanosilica

Table 1. Chemical components of cement and fly ash

| | Cement | Fly Ash |
|------------------------------------|--------|---------|
| CaO (%) | 63.67 | 5.43 |
| SiO ₂ (%) | 21.20 | 58.17 |
| Al ₂ O ₃ (%) | 5.23 | 26.34 |
| Fe ₂ O ₃ (%) | 3.57 | 8.11 |
| MgO (%) | 1.67 | 1.76 |
| SO ₃ (%) | 2.43 | 0.19 |
| Alkalis (%) | 2.23 | - |

Table 2. Physical characteristics of cement

| S. No. | Physical tests | Results |
|--------|----------------------|---------|
| 1. | Specific gravity | 3.14 |
| 2. | Consistency | 31% |
| 3. | Fineness | 2.67% |
| 4. | Soundness | 2.2 mm |
| 5. | Initial setting time | 35 min |
| 6. | Final setting time | 226 min |

Table 3. Physical characteristics of fly ash

| S. No. | Physical tests | Results |
|--------|------------------|---------|
| 1. | Specific gravity | 2.08 |
| 2. | pH | 7 |
| 3. | Moisture content | 2.4% |
| 4. | Colour | Grey |
| 5. | Shape | Round |

Table 4. Physical characteristics of M-sand

| S. No. | Physical tests | Results |
|--------|------------------|---------|
| 1. | Specific gravity | 2.75 |
| 2. | Fineness modulus | 4.65 |
| 3. | Water absorption | 6.6% |
| 4. | Surface texture | Smooth |
| 5. | Bulk density | 1.74 |
| 6. | Void ratio | 0.43 |
| 7. | Porosity | 0.33 |
| 8. | Zone | Zone 2 |

Table 5. Characteristics of PP

| S. No. | Particulars | Test Results |
|--------|-------------------|--------------------|
| 1. | Length | 6 mm |
| 2. | Diameter | 20 to 30 microns |
| 3. | Shape | Round |
| 4. | Specific gravity | 0.91 |
| 5. | Melting point | 160°C to 180°C |
| 6. | Tensile strength | 300 MPa to 400 MPa |
| 7. | Alkali resistance | Excellent |

2.2. M-Sand

M-sand was utilized as a fine aggregate. M-sand quality was evaluated in a laboratory using the guidelines of Indian standards. It helps in the improvement of strength and durability of mortar. The characteristics of M-sand determined through preliminary tests are listed in Table 4.

2.3. Polypropylene Fiber

The PP fiber, procured from BESCO fibers, India, was employed in this study. The characteristics of PP are listed in Table 5.

Table 6. The characteristics of nanosilica

| S. No. | Characteristics | Test Results |
|--------|-----------------|--------------|
| 1. | Colour | White |
| 2. | Form | Amorphous |
| 3. | Particle size | 10-20 nm |
| 4. | pH | 6.5-7.5 |

2.4. Nanosilica

The nanosilica employed in this study was purchased from Vedayukt, India. The characteristics of nanosilica are listed in Table 6. Figure 1 shows the nanosilica used in this study.

2.5 Accelerator

The accelerator Conplast NC was used here purchased from Fosroc, India. It obeys ASTM C-494 (Type C) and BS 5075 (Part 1). The characteristics of Conplast NC are listed in Table 7.

2.6 Mix Proportions

Table 8 shows different mix proportions of ECC mortar with 1 part of cement, 0.62 part of M-sand, 0.2 part of fly ash, 2% of PP, 0.8 part of accelerator and 0.18 part of water binder ratio with varying proportions of nanosilica at 0.05%, 0.1%, 0.15% and 0.2%.

Table 7. Characteristics of accelerator

| S. No. | Tests | Results |
|--------|------------------|-----------------------|
| 1. | Appearance | Straw coloured liquid |
| 2. | Specific gravity | 1.26 to 1.270 at 27°C |
| 3. | Freezing point | -16°C |
| 4. | Air entrainment | Less than 1% |
| 5. | Alkali content | Less than 155 g |

Table 8. Different mix proportions of ECC mortar

| Trail Mix | E1 | E1 | E1 | E1 |
|-------------|------|------|------|------|
| Cement | 1 | 1 | 1 | 1 |
| M-sand | 0.62 | 0.62 | 0.62 | 0.62 |
| Fly Ash | 0.2 | 0.2 | 0.2 | 0.2 |
| PP (%) | 2 | 2 | 2 | 2 |
| NS (%) | 0.05 | 0.1 | 0.15 | 0.2 |
| W/B | 0.18 | 0.18 | 0.18 | 0.18 |
| Accelerator | 0.8 | 0.8 | 0.8 | 0.8 |



Fig. 2: Set up of CS test

2.7 Specimen Preparations

The ECC mixtures were prepared using a mixing device. First, the powdered ingredients such as cement, fly ash, M-sand, and nanosilica were added and stirred for a minimum of 5 minutes. Then, water and accelerator were added to the dry mixture, and it was

blended for 5 to 7 minutes. Fibers were added to the wet mix in the last step. The fibers spread consistently after 3 to 6 minutes of distribution evenly. One of the benefits of mixing the ECC mix for longer than fifteen minutes is that the thixotropy effect is lessened (Krishnamoorthy *et al.* 2017).



Fig. 3: Set up of FS test

3. TESTS METHODOLOGY

3.1 Compressive Strength (CS) Test

Cube specimens with dimensions of $70.7 \times 70.7 \times 70.7$ mm were used to evaluate the CS of the ECC mixtures. According to the guidelines provided in IS 4031-Part 6: 1988, testing was done succeeding 3, 7, 14, and 28 days of curing. For every mixture, three samples were examined using a 200 kN compression testing machine, and then the average strength value was taken. Figure 2 shows the CS test setup.

3.2 Flexural Strength (FS) Test

Prism specimens with dimensions of $60 \times 25 \times 300$ mm were used to evaluate the FS of the ECC mixtures. Three-point bending testing was carried out after 7, 14, and 28 days of curing, in accordance with ASTM C78-15 recommendations. Figure 3 depicts the FS test setup.



Fig. 4: Set up of DTS test

3.3 Direct Tensile Strength (DTS) Test

In order to assess the DTS in ECC mixtures, dog bone specimens measuring 330 mm × 60 mm × 30 mm, an 80 mm gauge length, and a 30 mm × 30 mm cross-section were considered succeeding 7, 14, and 28 days of curing. A 100 kN universal testing equipment was used to perform the uniaxial DTS test. Figure 4 depicts the DTS test setup.

Table 9. Specification of pull-out testing mould

| Specification of mould | Size of mould in mm |
|-----------------------------|---------------------|
| Length | 110 |
| Breadth | 110 |
| Height | 130 |
| Thickness | 20 |
| Free space inside the mould | 20 |
| Supporting rod height | 325 |
| Diameter of supporting rod | 10 |

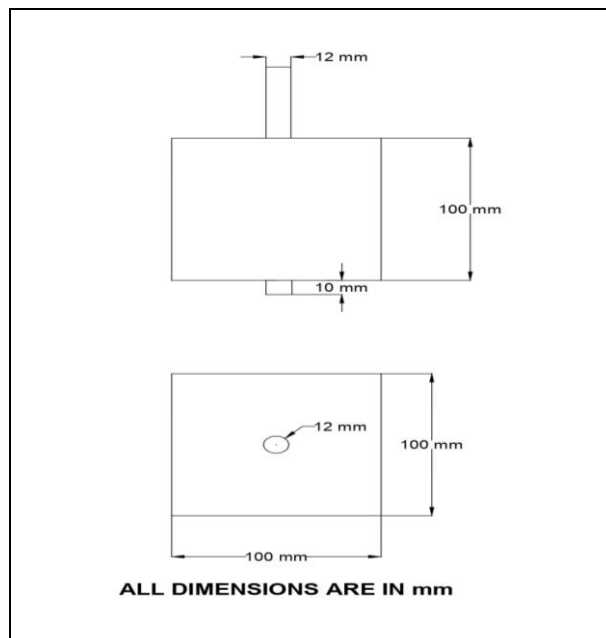


Fig. 5: POS test specimen



Fig. 6: Set up of POS test

3.4 Pull-Out Strength (POS) Test

The POS test was performed on ECC mixtures succeeding 28 days of curing, using the dimensions of a 100 × 100 × 100 mm cube, as per the IS: 2770 (Part 1) – 1967 code book. The diameter of the rod was 12 mm, and the thickness of the mould was 10 mm. The universal testing machine was used to test the specimens. Table 9 depicts the specifications of pull-out testing mould. Figure 5 depicts the pull-out specimen details. Figure 6 depicts the POS testing mould.

4. RESULTS AND DISCUSSION

4.1 CS Test

The results of CS of mortar with different NS contents are depicted in Fig.7. Figure 8 shows the compressive strength test after failure. Utilizing NS, the CS after 3 days of curing with NS contents of 0.05%, 0.1%, 0.15%, and 0.2% were 9.2 MPa, 9.5 MPa, 10.9 MPa, and 10.1 MPa, respectively. After 7 days of curing with same NS contents, the CS were 28.1 MPa, 29.5 MPa, 33.2 MPa, and 31.1 MPa, respectively. After 14 days of curing with same NS contents, the CS were 38.5 MPa, 43.7 MPa, 50.1 MPa, and 45.6 MPa, respectively. After 28 days of curing with same NS contents, the values were 49.2 MPa, 53.2 MPa, 57.3 MPa, and 54.4 MPa, respectively. The CS gradually increased with the increased percentage of NS content till 0.15% and suddenly decreased at 0.2% of NS content. The maximum values were observed at NS content of 0.15% and the minimum values at 0.05%.

Study with nano lime in ECC showed a maximum CS of 65 MPa with 4% nanolime (Khokhar *et al.* 2024). In contrast to the results reported, the current study demonstrated a decrease in CS. Study with the PVA and glass fibers showed a maximum CS of 54.1 MPa (Krishnaraja *et al.* 2022). In contrast to the results reported, the current study demonstrated an increase in compressive strength. These differences can be attributed to the variations in the materials, mix ratios, fibers used, nano material usage and the methodology applied in the current study in comparison to the prior ones.

An apparent increase in CS of ECC containing NS is noticed and NS is first added to improve strength by boosting compactness and hydration. However, as the amount of NS increases, issues such as agglomeration and excess of NS arise, which lowers the compressive strength. There is a threshold beyond which negative effects and diminishing returns become evident, and this is the ideal range for NS content in relation to strength enhancement (Zhang *et al.* 2022).

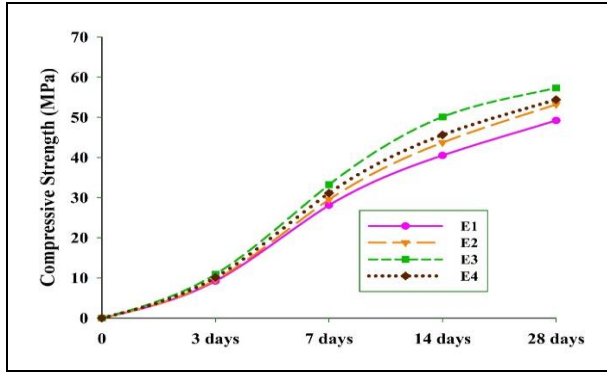


Fig. 7: CS of NS in investigated ECC

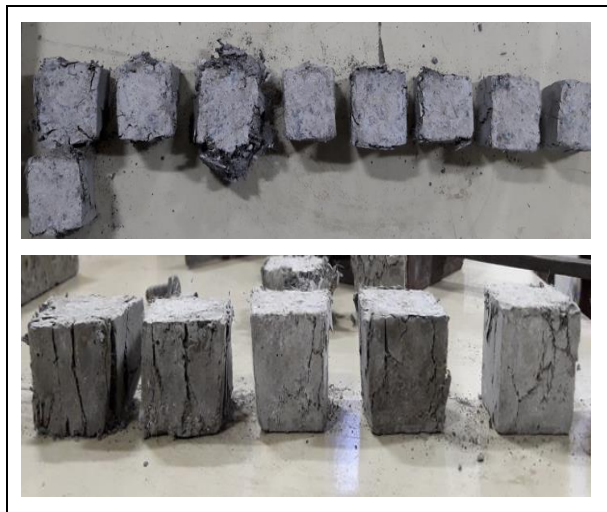


Fig. 8: CS test after failure

4.2 FS Test

The FS of mortar with different NS contents are depicted in Fig. 9. Figure 10 shows a flexural strength test after failure. Utilizing NS, the FS after 7 days of curing with NS contents 0.05%, 0.1%, 0.15%, and 0.2% were 5.4 MPa, 5.23 MPa, 6.97 MPa, and 6.45 MPa, respectively. After 14 days of curing with same NS contents, the FS were 14.9 MPa, 19.5 MPa, 23.4 MPa, and 21.7 MPa, respectively. After 28 days of curing with same NS contents, the FS were 20.2 MPa, 22.8 MPa, 27.5 MPa, and 24.6 MPa, respectively. The FS gradually increased with increase in NS content till 0.15% and suddenly decreased at 0.2% of NS content. The maximum values were observed at NS content of 0.15% and the minimum values at 0.05%.

A study with PVA and PP in ECC showed a maximum flexural strength of 24.3 MPa (Krishnaraja *et al.* 2018). In contrast to the results reported, the current study demonstrated an increase in compressive strength.

The incorporation of nanosilica in concrete enhanced flexural strength by acting as a filler. This resulted in improved cohesion within the material and the

creation of a denser microstructure. Additionally, the chemical reactivity of NS with calcium hydroxide crystals during hydration contributed to the formation of additional C-S-H gel, reinforcing the interfacial transition zone (ITZ) between the cement paste and aggregates (Mohamed, 2016; Tran *et al.* 2024).

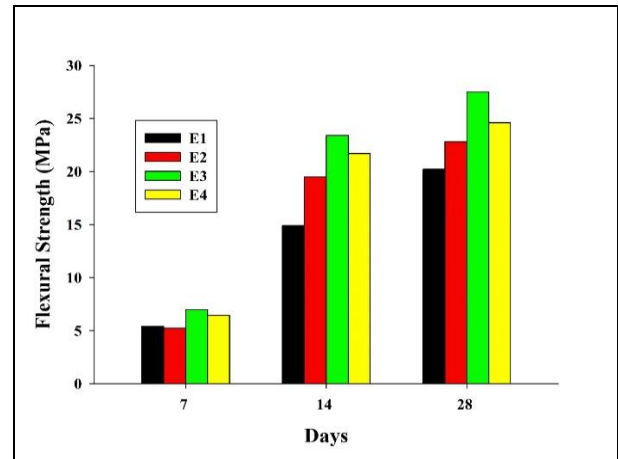


Fig. 9: FS of NS in investigated ECC



Fig. 10: FS test after failure

4.3 DTS Test

The DTS of mortar with different NS contents are depicted in Fig.11. Figure12 shows a tensile strength test after failure. Utilizing NS, the DTS after 7 days of curing with NS contents of 0.05%, 0.1%, 0.15%, and

0.2% were 1.7 MPa, 2 MPa, 2.5 MPa, and 2.3 MPa, respectively. After 14 days of curing with same NS contents, the DTS were 2.8 MPa, 3.2 MPa, 4.7 MPa, and 4.1 MPa, respectively. After 28 days of curing with same NS contents, the DTS were 5.1 MPa, 6.8 MPa, 7.9 MPa, and 7.2 MPa, respectively. The DTS gradually increased with the increased percentage of NS content till 0.15% and suddenly decreased at 0.2% of NS content. The maximum values were observed at NS content of 0.15% and the minimum values at 0.05%.

A recent study with nano calcium carbonate (NCC) showed a maximum DTS of 1.45 MPa at 2% of NCC (Liu et al. 2023). Study with PVA and steel fibers showed a maximum value of 7.6. In contrast to the results reported, (Krishnaraja et al. 2017) the current study demonstrated an increase in tensile strength. These differences can be attributed to variations in the all the experimental factors.

Incorporating NS in concrete significantly enhances splitting tensile strength, surpassing standard and supplementary materials. Nanosilica reduces pores, strengthens the interfacial transition zone, and contributes to early-phase strength gain (Althoey et al. 2023).

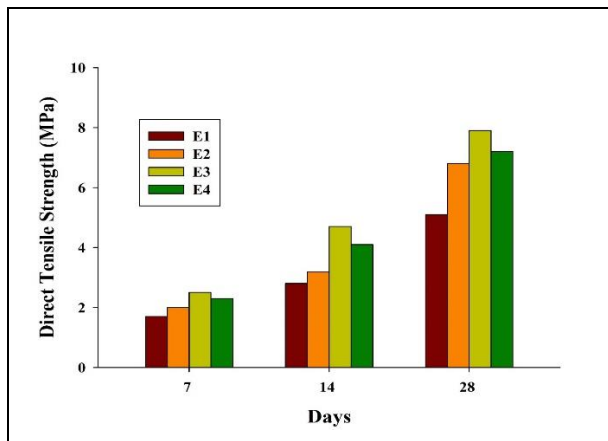


Fig. 11: DTS of NS in investigated ECC



Fig. 12: DTS test after failure

4.4 POS Test

The POS of mortar with different NS contents are listed in Table 10. Figure 13 shows a pull-out strength test after failure. Utilizing NS, the pull-out strength after 28 days of curing with NS contents of 0.05%, 0.1%, 0.15%, and 0.2% were: load at 0.25 mm slip ranging between 11.8kN and 17.3kN, stress at 0.25 mm slip ranging between 4.3N/mm² and 8.09N/mm², ultimate bond strength ranging between 15.64kN and 23.98kN, and ultimate bond stress ranging between 5.12N/mm² and 10.75N/mm². The pull-out strength gradually increases with increase in NS content till 0.15% and suddenly decreases at 0.2% of NS content. The maximum values were observed at NS content of 0.15 % and the minimum values at 0.05%.

In contrast to the results reported (Halvaei et al. 2013; Li et al. 2023; Oh et al. 2022), the current study demonstrated an increase in pull-out strength.

Table 10. The pull-out strength of mortar with different NS contents

| Mix | Load at 0.25 mm Slip (kN) | Stress at 0.25 mm Slip (N/mm ²) | Ultimate Bond Strength (kN) | Ultimate Bond Stress (N/mm ²) |
|-----|---------------------------|---|-----------------------------|---|
| E1 | 11.8 | 4.30 | 15.64 | 05.12 |
| E2 | 12.9 | 5.40 | 18.47 | 06.39 |
| E3 | 17.3 | 8.09 | 23.98 | 10.75 |
| E4 | 14.9 | 6.50 | 20.34 | 08.59 |



Fig. 13: POS test after failure

5. CONCLUSIONS

The study utilized NS for enhancing the performance of 3DP mortar printing and examined the improved qualities of the mortar. The following conclusions are derived.

1. Incorporating NS significantly improved the compressive, flexural, split tensile, and pull-out strength of ECCs.
2. Optimal NS content for peak mechanical performance was 0.15%, maximizing compressive, flexural, split tensile, and pull-out strength.
3. Exceeding optimum NS content, especially at 0.2%, led to a decline in mechanical properties, indicating challenges like agglomeration and dispersion issues.
4. Careful NS content selection, specifically at 0.15%, maximizes mechanical properties without compromising the performance of ECC.
5. Trends in compressive, flexural, split tensile, and pull-out strength offer insights for optimizing ECC formulations and advancing high-performance 3DP technologies.

FUNDING

This research received no specific grant from any funding agency in the public, commercial, or not-for-profit sectors.

CONFLICTS OF INTEREST

The authors declare that there is no conflict of interest.

COPYRIGHT

This article is an open-access article distributed under the terms and conditions of the Creative Commons Attribution (CC BY) license (<http://creativecommons.org/licenses/by/4.0/>).



REFERENCES

Afroughsabet, V. and Teng, S., Experiments on drying shrinkage and creep of high performance hybrid-fiber-reinforced concrete, *Cem. Concr. Compos.*, 106, 103481 (2020). <https://doi.org/10.1016/j.cemconcomp.2019.103481>

Althoey, F., Zaid, O., Martínez, G. R., Alsharari, F., Ahmed, M. and Arbili, M. M., Impact of Nano-silica on the hydration, strength, durability, and microstructural properties of concrete: A state-of-the-art review, *Case Stud. Constr. Mater.*, 18, e01997 (2023).

<https://doi.org/10.1016/j.cscm.2023.e01997>

Buswell, R. A., Da, S. W. L., Bos, F. P., Schipper, H. R., Lowke, D., Hack, N., Kloft, H., Mechtcherine, V., Wangler, T. and Roussel, N., A process classification framework for defining and describing Digital Fabrication with Concrete, *Cem. Concr. Res.*, 134, 106068 (2020).

<https://doi.org/10.1016/j.cemconres.2020.106068>

Elkady, H., Serag, M. I. and Elfeky, M. S., Effect of nano silica de-agglomeration, and methods of adding super-plasticizer on the compressive strength, and workability of nano silica concrete, *Civ. Environ. Res.*, 3(2), 21-34 (2013).

Eštoková, A., Wolfová Fabiánová, M. and Ondová, M., Concrete structures and their impacts on climate change and water and raw material resource depletion, *Int. J. Civ. Eng.*, 20(6), 735-747 (2022).

<https://doi.org/10.1007/s40999-022-00701-8>

Fang, B., Hu, Z., Shi, T., Liu, Y., Wang, X., Yang, D., Zhu, K., Zhao, X. and Zhao, Z., Research progress on the properties and applications of magnesium phosphate cement, *Ceram. Int.*, 49(3), 4001-4016 (2023).

<https://doi.org/10.1007/s12205-023-0623-x>

Ferdinánd, M., Várdai, R., Lummerstorfer, T., Pretschuh, C., Gahleitner, M., Faludi, G., Móczó, J. and Pukánszky, B., Impact modification of PP with short PET fibers: Effect of heat setting on fiber characteristics and composite properties, *Compos. Struct.*, 311, 116810 (2023).

<https://doi.org/10.1016/j.compstruct.2023.116810>

Halvaei, M., Jamshidi, M., Latifi, M. and Behdouj, Z., Performance of low modulus fibers in engineered cementitious composites (ECCs): flexural strength and pull out resistance, *Adv. Mater. Res.*, 687, 495-501 (2013).

<https://doi.org/10.4028/www.scientific.net/AMR.687.495>

Huang, H., Li, M., Yuan, Y. and Bai, H., Experimental research on the seismic performance of precast concrete frame with replaceable artificial controllable plastic hinges, *J. Struct. Eng.*, 149(1), 04022222 (2023).

<https://doi.org/10.1061/jsendh.steng-11648>

Ji, J., Zhang, Z., Lin, M., Li, L., Jiang, L., Ding, Y. and Yu, K., Structural application of engineered cementitious composites (ECC): A state-of-the-art review, *Constr. Build. Mater.*, 406, 133289 (2023).

<https://doi.org/10.1016/j.conbuildmat.2023.133289>

Khokhar, S. A., Ahmed, T., Khushnood, R. A., Basit, M. U. and Javed, S., Development of low carbon engineered cementitious composite (ECC) using nano lime calcined clay cement (nLC3) based matrix, *Case Stud. Constr. Mater.*, 20, e02669 (2024). <https://doi.org/10.1016/j.cscm.2023.e02669>

- Krishnamoorthy, M., Tensing, D., Sivaraja, M. and Krishnaraja, A. R., Durability studies on polyethylene terephthalate (PET) fibre reinforced concrete, *Int. J. Civ. Eng. Technol.*, 8(10), 634-640 (2017).
- Krishnaraja, A. R. and Kandasamy, S., Flexural performance of engineered cementitious compositelayered reinforced concrete beams, *Arch. Civ. Eng.*, 63(4), 173-189 (2017). <http://dx.doi.org/10.1515/ace-2017-0048>
- Krishnaraja, A. R., Anandakumar, S. and Jegan, S. M., Mechanical performance of hybrid engineered cementitious composites, *Cement Wapno Beton*, 23(6), 479-486 (2018).
- Krishnaraja, A. R., Harihanandh, M. and Anandakumar, S., Mechanical performance of engineered cementitious composites developed with different modulus fibers, *Cement Wapno Beton*, 26(6), 493-502 (2022).
- Li, F., Liu, G., Liu, M., Yang, Z., Chen, Z., Wen, T., Guo, J. and Shao, J., Investigations on influences of Engineered Cementitious Composites (ECC) on pull-out properties of studs in steel-concrete composite bridge, *Case Stud. Constr. Mater.*, 18, e02131 (2023). <https://doi.org/10.1016/j.cscm.2023.e02131>
- Liu, Q., Jiang, Q., Zhou, Z., Xin, J. and Huang, M., The printable and hardened properties of nano-calcium carbonate with modified polypropylene fibers for cement-based 3D printing, *Constr. Build. Mater.*, 369, 130594 (2023). <https://dx.doi.org/10.2139/ssrn.4217565>
- Lu, M., Xiao, H., Liu, M., Li, X., Li, H. and Sun, L., Improved interfacial strength of SiO₂ coated carbon fiber in cement matrix, *Cem. Concr. Compos.*, 91, 21-28 (2018). <https://doi.org/10.1016/j.cemconcomp.2018.04.007>
- Malchiodi, B., Pelaccia, R., Pozzi, P. and Siligardi, C., Three sustainable polypropylene surface treatments for the compatibility optimization of PP fibers and cement matrix in fiber-reinforced concrete, *Ceram. Int.*, 49(14), 24611-24619 (2023). <https://doi.org/10.1016/j.ceramint.2023.02.105>
- Mohamed, A. M., Influence of nano materials on flexural behavior and compressive strength of concrete, *HBRC journal*, 12(2), 212-225 (2016). <https://doi.org/10.1016/j.hbrj.2014.11.006>
- Nazar, S., Yang, J., Amin, M. N., Husnain, M., Ahmad, F., Alabduljabbar, H. and Deifalla, A. F., Investigating the Influence of PVA and PP Fibers on the Mechanical, Durability, and Microstructural Properties of One-Part Alkali-Activated Mortar: An Experimental Study, *J. Mater. Res. Technol.*, 25, 3482-3495 (2023). <https://doi.org/10.1016/j.jmrt.2023.06.115>
- Oh, T., Chun, B., Lee, S. K., Lee, W., Banthia, N. and Yoo, D. Y., Substitutive effect of nano-SiO₂ for silica fume in ultra-high-performance concrete on fiber pull-out behavior, *J. Mater. Res. Technol.*, 20, 1993-2007 (2022). <https://doi.org/10.1016/j.jmrt.2022.08.013>
- Sun, J., Aslani, F., Wei, J. and Wang, X., Electromagnetic absorption of copper fiber oriented composite using 3D printing, *Constr. Build. Mater.*, 300, 124026 (2021). <http://dx.doi.org/10.1016/j.conbuildmat.2021.124026>
- Tran, H. B. and Phan, V. T. A., Potential usage of fly ash and nano silica in high-strength concrete: laboratory experiment and application in rigid pavement, *Case Stud. Constr. Mater.*, 20(12), e02856 (2024). <http://dx.doi.org/10.1016/j.cscm.2024.e02856>
- Várdai, R., Lummerstorfer, T., Pretschuh, C., Jerabek, M., Gahleitner, M., Faludi, G., Móczó, J. and Pukánszky, B., Reinforcement of PP with polymer fibers: Effect of matrix characteristics, fiber type and interfacial adhesion, *Polym.*, 190, 122203 (2020). <https://doi.org/10.1016/j.polymer.2020.122203>
- Wan, Q., Yang, W., Wang, L. and Ma, G., Global continuous path planning for 3D concrete printing multi-branched structure, *Addit. Manuf.*, 71, 103581 (2023). <https://doi.org/10.1016/j.addma.2023.103581>
- Wasim, M., Abadel, A., Bakar, B. A. and Alshaikh, I. M., Future directions for the application of zero carbon concrete in civil engineering—A review, *Case Stud. Constr. Mater.*, 17(2), e01318 (2022). <http://dx.doi.org/10.1016/j.cscm.2022.e01318>
- Wu, Z., Khayat, K. H. and Shi, C., Effect of nano-SiO₂ particles and curing time on development of fiber-matrix bond properties and microstructure of ultra-high strength concrete, *Cem. Concr. Res.*, 95(2), 247-256 (2017). <http://dx.doi.org/10.1016/j.cemconres.2017.02.031>
- Yang, Z., He, R., Tan, Y., Chen, H. and Cao, D., Air pore structure, strength and frost resistance of air-entrained mortar with different dosage of nano-SiO₂ hydrosol, *Constr. Build. Mater.*, 308, 125096 (2021). <http://dx.doi.org/10.1016/j.conbuildmat.2021.125096>
- Zhang, H., Wu, Z., Hu, X., Ouyang, X., Zhang, Z., Banthia, N. and Shi, C., Design, production, and properties of high-strength high-ductility cementitious composite (HSHDCC): A review, *Composites, Part B*, 110258 (2022). <https://doi.org/10.1016/j.compositesb.2022.110258>
- Zhang, M., Zhu, X., Liu, B., Shi, J., Gencel, O. and Ozbakkaloglu, T., Mechanical property and durability of engineered cementitious composites (ECC) with nano-material and superabsorbent polymers, *Powder Technol.*, 409, 117839 (2022). <https://doi.org/10.1016/j.powtec.2022.117839>
- Zhang, R. C., Wang, L., Xue, X. and Ma, G. W., Environmental profile of 3D concrete printing technology in desert areas via life cycle assessment, *J. Cleaner Prod.*, 396, 136412 (2023).